



FAILURE ENVELOPE OF THE BRITTLE STRENGTH OF ICE IN THE FIXED-END BEAM TEST (TWO SCENARIOS)

Alexander Sakharov¹, Evgeny Karulin², Aleksey Marchenko^{3,4}, Marina Karulina², Devinder Sodhi⁵ and Peter Chistyakov¹

¹ *Moscow State University, Moscow, Russia*

² *Krylov State Research Centre, St.-Petersburg, Russia*

³ *The University Centre in Svalbard, Longyearbyen, Norway*

⁴ *Sustainable Arctic Marine and Coastal Technology (SAMCoT), Centre for Research-based Innovations (CRI), Norwegian University of Science and Technology, Trondheim, Norway*

⁵ *Retired from Cold Region Research Engineering Laboratory, Hanover, NH, USA*
asakh@rambler.ru

Abstract

Two types of full-scale, in situ tests were conducted in Van Mijen Fiord in March 2013, Barents Sea in May 2013 and Lyb Lake in November 2014. Tests conducted were: (a) cantilever beam tests to determine flexural strength and (b) fixed-end beam tests to determine flexural and compressive strengths. The results of these tests are presented here. Short-term loading of floating ice sheets to failure was investigated. The focus was on flexural strength of the first-year sea ice and fresh water ice. To determine flexural strength cantilever beam tests for a wide range of length-to-thickness ratio L/h were conducted. In fixed-end beam tests two different failure modes have been observed. For ratio $L/h > 6$, initial bending mode of fixed-end beam transform to equilibrium of block structure after propagation of cracks in the center and the roots of a fixed-end beam. The equilibrium of block structure is provided by wedging action as proposed by Sodhi (1998). We present two approaches to explore the transition from the whole beam to block structure: (1) numerical simulation, and (2) full-scale measurements in field tests.

For $L/h < 6$ other failure scenario takes place. The cracks break a centre-edge ice block from the beam. This failure type, named punch effect, is a brittle failure in shear. In this case the crushing can be attributed to shear failure envelope in compressive-tensile quadrant (Schulson *et al*, 1999, 2006). Results of the numerical transition simulation, the stress distributions in vertical, horizontal and diagonal planes of the ice beam are presented for various L/h ratio. Also, the brittle failure mechanism is discussed.

1. Introduction

Investigations of the sea ice mechanical properties in the field have lead to opportunities to measure not only the crushing load and displacement but also to observe different fracture scenarios and failure modes. It provides us with opportunities to formulate failure criteria for full-scale objects and to check if they correlate with results for small-scale simulation in the ice basin and in laboratory tests.

Tests with cantilever beam are very important to determine σ_f flexural strength of the sea and fresh water ice. The results are used for calculation of ice loads sloping structures and ships

(Vaudray, 1977, Schwarz *et al*, 1981), as well as for estimation of bearing capacity of floating ice and surface wave amplitudes, which potentially could break up the floating ice (Frederking and Svec, 1985; Dumont *et al*, 2011).

Tests with in situ fixed-end beam are performed to determine compressive strength of floating ice (Sodhi, 1998). The results are used to estimate breakthrough load of floating ice sheets, which are often used as construction and transportation platforms. We started conducting tests with fixed-end beam for fresh and saline ice in 2012. It was done in the same places as tests with cantilever beam. Since 2013 these tests have been carrying out not only with vertical but also with horizontal load upon the beam. in this case failure modes it is easy to observe.

Two different equilibrium modes take place: bending mode (Fig. 1a) and block structure mode (Fig. 1b). The second mode follows after flexural stress is equal to flexural strength and propagation of cracks at the center and the roots of the beam.

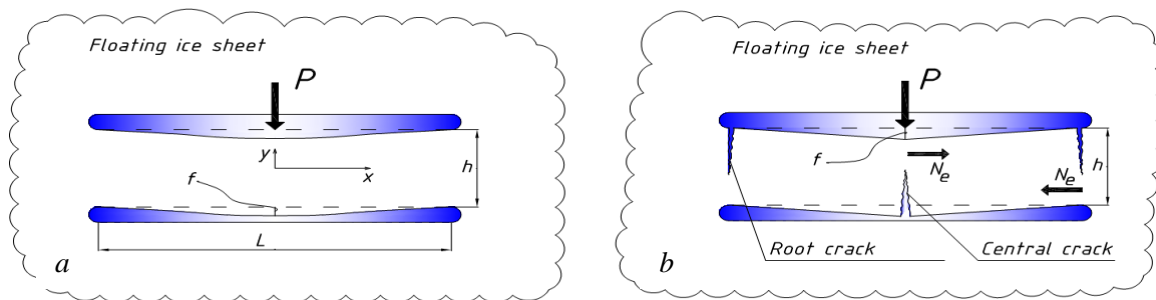


Figure 1. Two equilibrium modes of the fixed-end beam under applied load P , (a) – bending mode, (b) – block structure mode with wedging action (Sodhi's scenario)

Specific type of load-displacement curve where the bending mode transitioned to block structure mode was observed in both laboratory experiments and field tests (Marchenko *et al*, 2014). This transition from one equilibrium mode to another, named Sodhi's scenario, is due to wedging action. That's why wedging action is of interest and we investigated it for different scenario of cracks propagation in a wide range of beam ratio L/h . In the present paper the transition from bending mode to block structure mode is investigated. The results of numerical simulation of this transition are presented below.

In some tests with fixed-end beam we observed another scenario. The beam is broken by diagonal cracks which extend from the point of load application to beam roots (Fig. 2a). This failure type where a centre-edge ice block is separated by cracks is named punch effect. It can be observed in tests with saline and fresh water ice for fixed-end beam length-to-thickness ratio $L/h < 4$ for both horizontal and vertical loading. In case when $4 < L/h < 6$ we could see a combined failure mode (Fig.2b)- some combinations of the two scenarios.

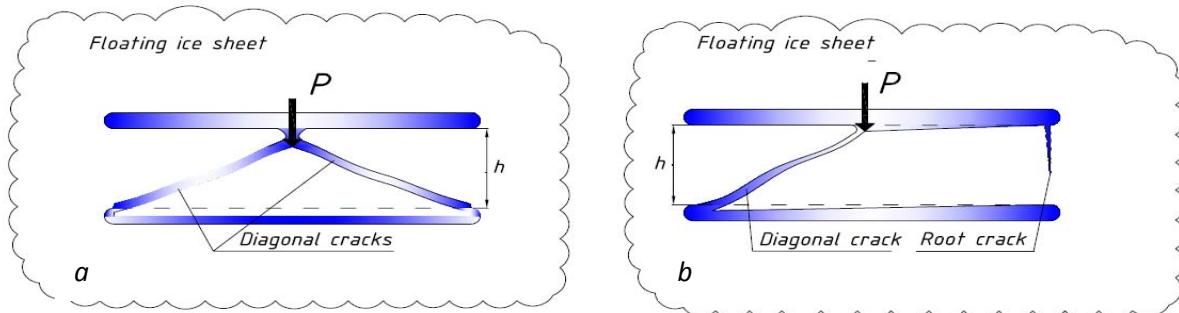


Figure 2. Punch effect in fixed-end beam test, (a) – punch effect, (b) – combined failure mode

In the present paper the results of numerical simulation and stress distributions of an ice beam with cracks are used to analyze the brittle failure mode in fixed-end beam tests.

2.The transition from bending mode to block structure mode (numerical simulation).

In experiments on tensile strength of the sea ice (Richter-Menge and Jones, 1993) the failure of all samples was brittle, but pure elastic behavior was discovered only when strain rate was more than 10^{-3}s^{-1} . Nonlinear or plastic deformation portion was up to 20% of the total deformation for the strain rate 10^{-5}s^{-1} and less. Therefore we assume that plastic deformation portion in our tests is less than 20% and use of linear elastic model for the numerical analysis is justified.

Numerical simulation of the test was performed in SCAD v7.31 for linear elastic mode. The fixed-end beam tests under horizontal and vertical loading were simulated by FEM analysis. The cracks were simulated by different length cuttings. The stress-strain distributions in vertical, horizontal and diagonal planes of the beam were considered. As a result of this analysis, confined (or wedging) force is calculated using formula

$$N_e = \int_0^b \int_{-h/2}^{h/2} \sigma_{xx} dz dy, \quad (1)$$

where b, h – width and height of the beam, σ_{xx} – normal stresses in vertical plane. The confined force N_e is the reaction force due to the effect of beam confining by surrounded material. In Tables 1-3 the values of confined force N_e and displacement are performed for various beam sizes.

Table 1. Medium size beam ($L=5.0$; $h=0.5$; $b=0.4$ m), $P=88.3$ kN

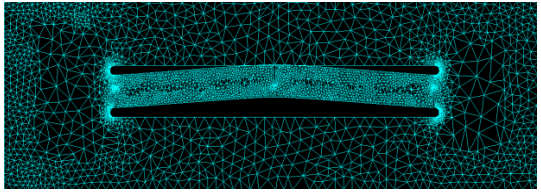
Model	Displacement f , mm	Confined force, N_e , kN	Sketch
Without cracks	17.7	0.7	
Root cracks, $L_c=25\text{cm}$	27.4	95.1	
Central crack, $L_c=25\text{cm}$	25.1	132.3	
Central and root cracks, $L_c=25\text{cm}$	36.,4	204.6	
Central and root cracks, $L_c=30\text{cm}$	42.6	224.7	

Table 2. Short beam ($L=2.0$; $h=0.5$; $b=0.4$ m), $P=88.3$ kN

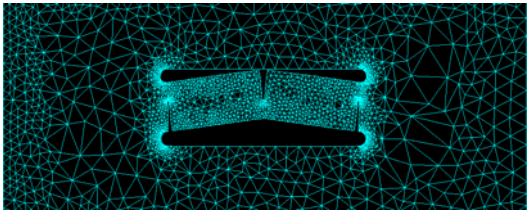
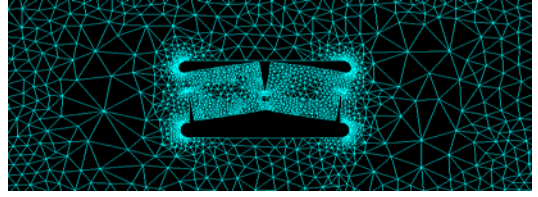
Model	Displacement f , mm	Confined force, N_e , kN	Sketch
Without cracks	2.1	1.0	
Root cracks, $L_c=25\text{cm}$	3.1	43.3	
Central and root cracks, $L_c=25\text{cm}$	2.7	83.3	
Central and root cracks, $L_c=30\text{cm}$	4.8	100.7	

Table 3. Very short beam ($L=1.25$; $h=0.5$; $b=0.4$ m), $P=88.3$ kN

Model	Displacement f , mm	Confined force, N_e , kN	Sketch
Without cracks	1.1	1.4	
Root cracks, $L_c=20$ cm	1.4	29.7	
Root cracks, $L_c=30$ cm	1.6	32.2	
Central and root cracks, $L_c=30$ cm	1.8	69.7	

Analyzing the results of numerical simulation, the transition from bending mode to block structure mode for ratio ($2.5 \leq L/h \leq 10$) we conclude the following.

- The influence of the crack length on relative stiffness of the beam is not significant; the shorter beam, the smaller influence is.
- The value of confined force N_e in bending mode is small, N_e/P is less than 5% and can be neglected. In transition, the force N_e increases rapidly, as a result of the cracks growth, especially the central crack growth. In the end of transition the confined force N_e remains the only internal factor which supports the block structure equilibrium under applied load.
- Stress concentration in the beam root (Svec *et al*, 1981, 1985) is the reason that when a beam is loaded by horizontal load first cracks appear in the root area. After appearing the cracks are increasing in size only in tension area in a half-height of the beam. The crack in the central area appears almost simultaneously after the stress distribution has changed. If the beam is loaded by vertical force, the crack in the central part appears the first and root cracks follow (Marchenko *et al*, 2014).
- Further cracks grow until the crack tips reach compression area (approximately 3/5 thickness of the beam).

The decrease in the stiffness $k_0 = \frac{dP_0(f)}{df} > k_i > k_w = \frac{dP_w(f)}{df}$ is connected with breaking down of the beam material due to central and root cracks propagation. The transition is illustrated by the load-displacement graph of the fixed-end beam test numerical simulation (Fig. 3)

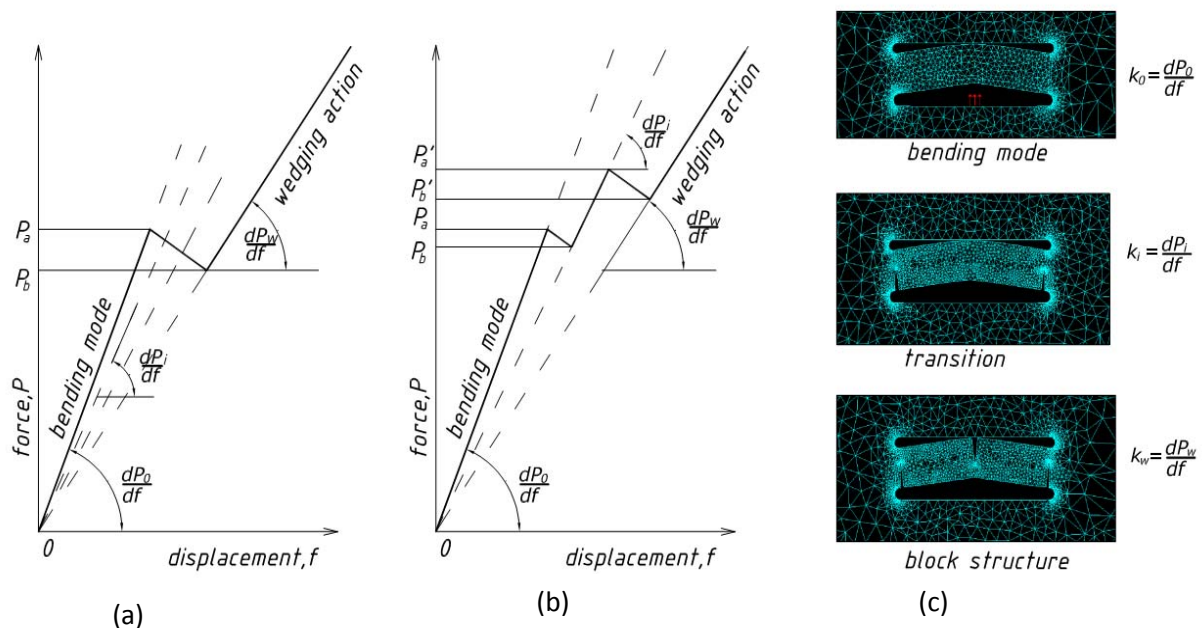


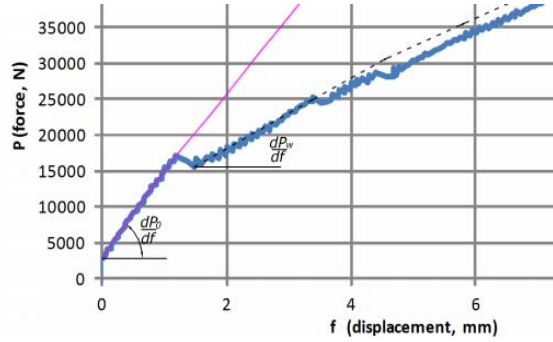
Figure 3. Transition from bending mode to block structure in one step (a), in several steps (b), in numerical analysis (c). P_a -load of transition

3. The transition from bending mode to block structure mode (full-scale test).

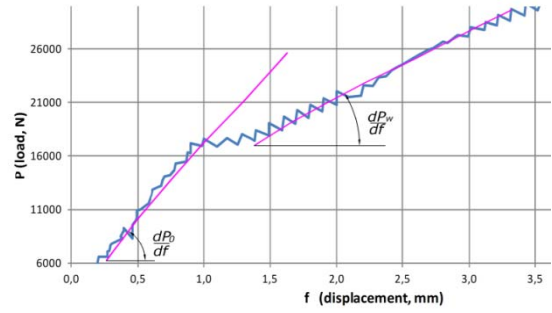
Full-scale, fixed-end beam tests were conducted with both saline and fresh water (lake) ice during the period of 2013-2014 in Svalbard. We analyzed the data from fixed-end beam tests and tried to distinguish the transition (Fig 4a...4d). Carrying capacity of fixed-end beam under the short-term loading is higher than transition load value P_a . Formula for the calculation P_a

$$P_a = \frac{4\sigma_f b h^2}{3L} \quad (2)$$

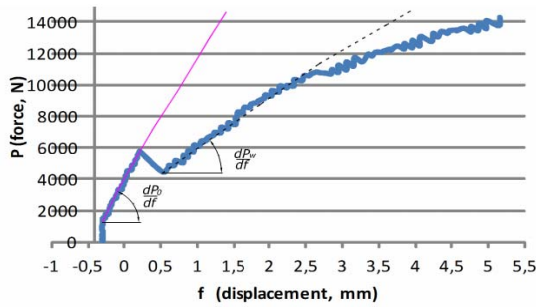
is valid when the transition is following Sodhi's scenario (Fig 1b).



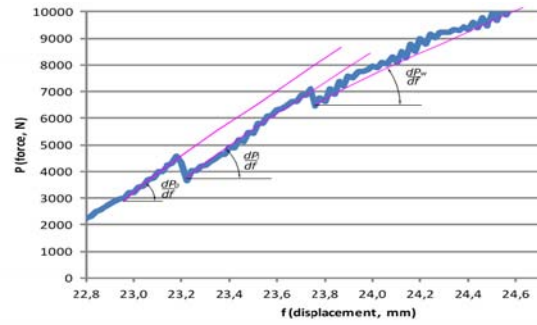
(a) sea ice (Van-Mijen fiord, 09_March_2013, $h_{ice}=0.73m$)



(b) sea ice (Van-Mijen fiord, 14_March_2013, $h_{ice}=0.76m$)



(c) lake ice (Lake Lyb, 25_Oct_2014, $h_{ice}=0.27m$)



(d) lake ice (Lake Lyb, 27_Oct_2014, $h_{ice}=0.25m$)

Figure 4. Detailed transition area of load-displacement graph of the fixed-end beam test (vertical loading)

Table 4. Data test analysis (Relative stiffness)

Fig.	Dimension of the beam, $(L*b*h, m)$	Type of ice	P_a , kN	P_b , kN	$k_0 = \frac{dP_0(f)}{df}$, kN/mm	$k_w = \frac{dP_w(f)}{df}$, kN/mm	$\frac{k_w}{k_0}$
4a	7.0*0.72*0.73	Sea ice	16.3	15.5	12.2	5.3	0.43
4b	7.0*0.64*0.76	Sea ice	17.6	16.9	13.9	5.8	0.42
4c	4.1*0.6*0.27	Lake ice	5.8	4.5	9.2	3.0	0.33
4d	4.2*0.58*0.25	Lake ice	4.3	3.7	7.6	3.9	0.51

The relative stiffness of fixed-end beam with ratio $L/h=10$ in the numerical simulation the transition is equal $\frac{k_w}{k_0} = \frac{17.7}{42.6} = 0.41$ (Table 2), which is in a good agreement with the test data

Table 4 (4a, 4b).

In transition $P_a \rightarrow P_b$ the stored mechanical energy of the system «ice beam-power rig» is spent on cracks propagation. From tests data we can evaluate acceleration and inertia forces in the transition. From load-displacement graph (Fig. 4a) time interval is $\Delta t = t_b - t_a = 0.06s$ and variation of displacement is $\Delta f = f_b - f_a = 0.32mm$, thus the acceleration value is estimated to be $a \approx \frac{\Delta f}{(\Delta t)^2} = 0.089ms^{-2}$ and the inertial force are estimated to be small, leading to a quasi-static process. It can be interpreted as meso-scale model for material damage theory (Bazant, 2002).

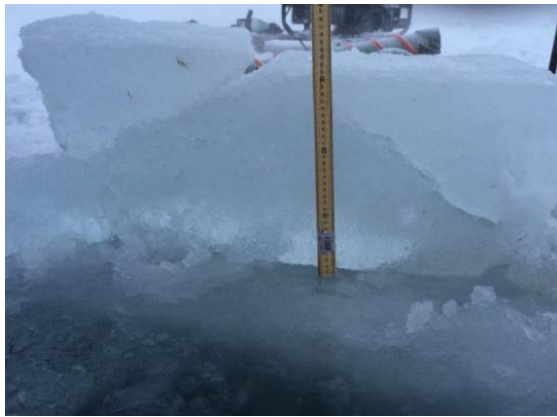
4. Punch effect in fixed-end beam tests.

Main goal of the test with fixed-end beam is the calculation of the compressive strength of floating ice in full scale and natural environment. The compressive strength of ice σ_c determines the carrying capacity of fixed-end beam due to wedging action using Sodhi (1998) formula

$$P_{\max} = \frac{4\beta(1-\beta)\sigma_c b h^2}{L}, \quad \beta \cong 1/3 \quad (3)$$

Punch effect is an alternative to Sodhi's scenario and can be observed in full-scale sea ice and fresh water ice fixed-end beam tests for both horizontal and vertical loading.

As mentioned above, punch effect can be observed in tests (Fig.5) with the fixed-end beam with ratio $L/h < 4$. It has been never been observed in tests with ratio $L/h > 6$. In case when $4 < L/h < 6$ we could see a combined failure mode.



(a)



(b)

Figure 5. Punch scenario in-situ tests, (a) – vertical loading (Lyb Lake, 29_Oct_2014), (b) – horizontal loading (Lyb Lake, 28_Oct_2014)

The diagonal crack propagates in the ice through the pure shear beam zone. The principal stresses are almost equal in values and have opposite signs – compression in diagonal and tension in orthogonal direction. The fracture we could watch in tests is in accordance with failure envelope in compressive-tensile quadrant (Fig.6). The shear strength of ice τ_s determines the carrying capacity of fixed-end beam due to punch effect.

$$P_p = 2k\tau_s b h, \quad k = k\left(\frac{L}{h}\right) \leq 1 \quad (4)$$

Linear elastic analysis of a beam model provides us with stress values in the beam roots or beam centre or diagonal planes. Correlating these values with the failure envelope, we were able to verify that the limit state in the beam roots or center occurs earlier than in diagonal planes. Nevertheless we faced punch effect in field tests in wider range of beam ratio. There are some suggestions to explain the differences between theory and test. Firstly, we suppose that the influence of stress concentrations in the contact area where the load is applied is essential (Morozov and Zernin, 1999). More detailed analysis in contact area vicinity shows that there is some local zone under contact pad within the beam with a high level of tension. It can be a trigger for further

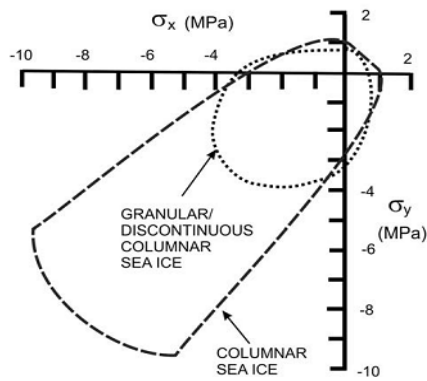


Fig. 6. Failure envelope (Schulson, 1999)

crack growth. Secondly, the investigation of the stress distribution in vicinity of the edge of the linear defect in beam shows the significant tension (Fig.7) in the pip of defect.

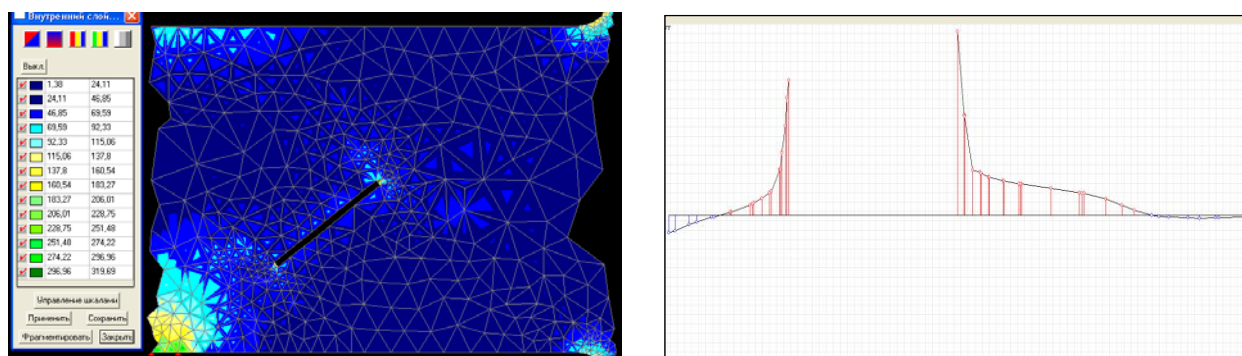


Figure 7. Stress distribution in vicinity of a linear defect in shear beam zone; FEM analysis of the beam with a linear defect and peaks of tension at the tip of a linear defect

Taking the above into account we would like to mention that there is a need to investigate this failure mode of a short ice beam.

5. Conclusion.

The fixed-end beam tests give a lot of data to determine mechanical parameters such as flexural, compression and shear strength of ice in full scale and natural environment. For safety of maritime operations, these are the most important parameters design of safe coastal structures. These tests

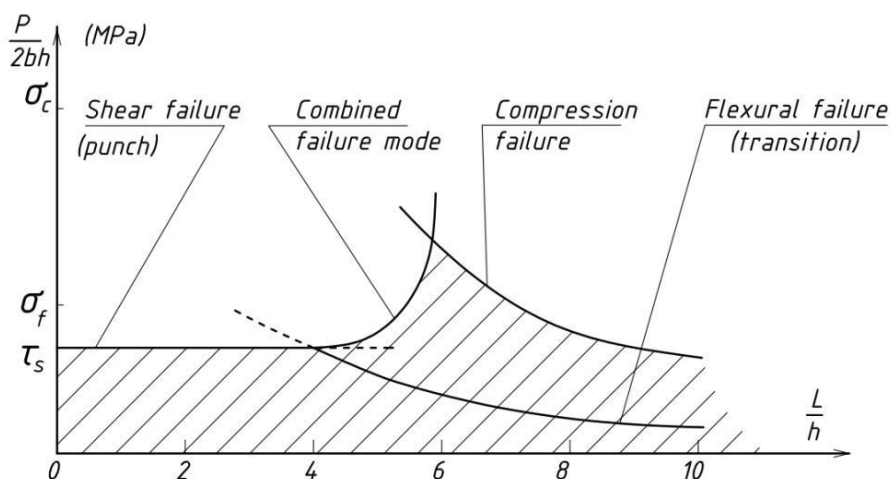


Figure 8. Diagrams of failure modes

give opportunities not only to measure the crushing forces but also to observe different fracture scenarios to work out more realistic failure schemes. The diversity of failure modes is represented on failure envelope of an ice beam (Fig.8). Shaded area on the graph corresponds to those the values of parameters which ensure carrying capacity of fixed-end

beam. The border of this area consists of different parts of curves representing various failure modes determined by formulas (2) – (4). The two alternative scenarios (shear failure and compression failure) are separated by combined failure mode. Transition plays a specific role. Transition from bending mode equilibrium to block structure equilibrium initiates the appearing and growth of central and root beam cracks and thus punching of a centre-edge ice block becomes impossible. The transition is a sequence of unstable configurations as a result of brittle failure mechanism. In this process confined (or wedging) forces grow rapidly and change finally the stress distribution. The result of transition simulation is in good agreement with full-scale tests data. The numerical simulation of punch effect is not adequate. So, further research of shear failure mode appears to be the front burner and necessary to the design practice.

Acknowledgement

Authors are grateful to UNIS for the funding of, and the logistic support for, field tests near Svea, Svalbard. The experimental equipment for field works has been designed and manufactured under support of SAMCoT project.

References

- Bazant, Z. P. 2002. Concrete fracture models: testing and practice. *Engineering Fracture Mechanics*, Vol. 69, No. 2, pp. 165–205.
- Dumont, D., Kohout, A., Bertino, L., 2011. A wave-based model for the marginal ice zone including a floe breaking parameterization. *Journal of Geophysical Research*, 116, C04001.
- Frederking, R.M.W., Svec, O.J. , 1985. Stress-relieving techniques for cantilever beam tests in an ice cover. *Cold Regions Science and Technology* 11:247-253.
- Marchenko, A., Karulin, E., Chistyakov, P., Sodhi, D., et al, 2014. Three dimensional fracture effects in tests in cantilever and fixed ends beams, 22nd IAHR International Symposium on Ice, Singapore, 7 pp.
- Morozov, E.M., Zernin M.V., 1999. Contact problems of fracture mechanics. Moscow, *Machinostroenie*, 544p. (in Russian)
- Richter-Menge, J.A., Jones, K.F., 1993. The tensile strength of first-year sea ice. *J. Glaciology*, 39(133): 609-618.
- Schwarz, J., Frederking, R., Gavrilov, V., Petrov, I.G., Hirayama, K.I., Mellor, M., Tryde, P. and Vaudry K.D., 1981. Standardized testing methods for measuring mechanical properties of sea ice. *Cold Regions Science and Technology* 4:245-253.
- Schulson, E.M., Duval, P., 2009. *Creep and Fracture of Ice*. Cambridge University Press, 417pp.
- Schulson, E.M., Fortt, A.L., Iliescu, D., Renshaw, C.E., 2006. Failure envelope of first-year Arctic sea ice: the role of friction in compressive fracture. *Journal of Geophysical Research* 111 (C11S25)
- Sodhi, D.S. (1998) Vertical penetration of floating ice sheets. *International Journal of Solids Structures*, 35 (31-32): 4275-4294.
- Svec, O.J., Frederking, R.M.W, 1981. Cantilever beam tests in an ice cover: Influence of plate effects at the root. *Cold Regions Science and Technology* 11: 93-101.
- Svec, O.J., Thompson, J.C. and Frederking, R.M.W., (1985) Stress-concentrations in the root of an ice cover cantilever: Model tests and theory. *Cold Regions Science and Technology* 11: 63-73.
- Vaudray, K.D., 1977. *Ice engineering: Study of related properties of floating sea-ice sheets and summary of elastic and viscoelastic analysis*. US Navy Civil Engineering Lab. Rept. TR-860. Port Hueneme, CA.